

Dynamical behavior of solitons of the perturbed nonlinear Schrödinger equation and microtubules through the generalized Kudryashov scheme

M. Ali Akbar^a, Abdul-Majid Wazwaz^b, Forhad Mahmud^c, Dumitru Baleanu^{d,e,f,*}, Ripan Roy^g, Hemonta Kumar Barman^h, W. Mahmoud^{j,*}, Mohammed A. Al Sharifⁱ, M.S. Osman^{i,j,*}

^a Department of Applied Mathematics, University of Rajshahi, Bangladesh

^b Department of Mathematics, Saint Xavier University, Chicago, IL 60655, USA

^c Department of Applied Mathematics, Noakhali Science and Technology University, Bangladesh

^d Department of Mathematics, Cankaya University, 06530 Ankara, Turkey

^e Institute of Space Sciences, Magurele, 077125 Bucharest, Romania

^f Department of Medical Research, China Medical University Hospital, China Medical University, Taichung, Taiwan

^g Department of Mathematics, Bangamata Sheikh Fojilatunnesa Mujib Science & Technology University, Bangladesh

^h Department of Computer Science and Engineering, University of Creative Technology Chittagong, Bangladesh

ⁱ Department of Mathematics, Faculty of Applied Science, Umm Al-Qura University, Makkah 21955, Saudi Arabia

^j Department of Mathematics, Faculty of Science, Cairo University, Giza 12613, Egypt

ARTICLE INFO

Keywords:

Kerr law nonlinearity
Nonlinear evolution equations
Soliton solutions
3D wave envelopes

ABSTRACT

The perturbed nonlinear Schrödinger (NLS) equation and the nonlinear radial dislocations model in microtubules (MTs) are the underlying frameworks to simulate the dynamic features of solitons in optical fibers and the functional aspects of microtubule dynamics. The generalized Kudryashov method is used in this article to extract stable, generic, and wide-ranging soliton solutions, comprising hyperbolic, exponential, trigonometric, and some other functions, and retrieve diverse known soliton structures by balancing the effects of nonlinearity and dispersion. It is established by analysis and graphs that changing the included parameters changes the waveform behavior, which is largely controlled by nonlinearity and dispersion effects. The impact of the other parameters on the wave profile, such as wave speed, wavenumber, etc., has also been covered. The results obtained demonstrate the reliability, efficiency, and capability of the implemented technique to determine wide-spectral stable soliton solutions to nonlinear evolution equations emerging in various branches of scientific, technological, and engineering domains.

Introduction

Studies of soliton solutions to nonlinear evolution equations (NLEEs) have become increasingly important in the analysis of nonlinear phenomena in recent years [1]. Soliton is a special form of solitary wave that travels by maintaining its outline, velocity, and amplitude. It has a number of interesting features that interprets various types of nonlinear incidents. NLEEs arise in diverse scientific fields, namely climatology, theoretical physics, chemistry, biology, optical pulses, technology of space, fluid dynamics, signal processing, laser technology, applied mathematics and computer engineering. There are some NLEEs that are used in a variety of applied science disciplines, as for instance, the

Maxwell equation in electromagnetism [2], the heat equation in thermodynamics [3], the voltage analysis in nonlinear electrical transmission lines [4], the Lotka-Volterra equation in biology [5], the highly dispersive Schrödinger equation in nonlinear optics [6], the Navier-Stokes equation in fluid dynamics [7], etc. These incidents are essentially modeled by NLEEs, and the exact solutions of respective instances deliver a significant contribution in the nonlinear field. It is notable that, there has some significant advancement in the analysis of explicit solutions in the current years. However, there is no unique method to examine all kind of NLEEs. Each equation has to be studied as a separate problem. For determining the exact solutions of individual problem, diverse group of mathematicians, physicists and engineers are working

* Corresponding authors at: Department of Mathematics, Cankaya University, 06530 Ankara, Turkey (D. Baleanu). Department of Mathematics, Faculty of Science, Cairo University, Giza 12613, Egypt (W. Mahmoud) Department of Mathematics, Faculty of Applied Science, Umm Al-Qura University, Makkah, 21955, Saudi Arabia (M.S. Osman).

E-mail addresses: dumitru@cankaya.edu.tr (D. Baleanu), mwael@cu.edu.eg (W. Mahmoud), msozman@uqu.edu.sa, mofatzi@cu.edu.eg (M.S. Osman).

<https://doi.org/10.1016/j.rinp.2022.106079>

Received 28 September 2022; Received in revised form 28 October 2022; Accepted 31 October 2022

Available online 1 November 2022

2211-3797/© 2022 The Author(s). Published by Elsevier B.V. This is an open access article under the CC BY-NC-ND license (<http://creativecommons.org/licenses/by-nc-nd/4.0/>).

simultaneously. Thus, several techniques for exploring analytic solutions have been established. Some of them are, the new extended FAN sub-equation method [8], the sine-Gordon expansion technique [9], the Hirota method [10], the (G'/G) -expansion technique [11], the fractional dual-function scheme [12], the Darboux transformation method [13], the generalized Kudryashov technique [14], the physics-informed neural network scheme [15], the residual power series technique [16], the Laplace-Adomian decomposition approach [17], the finite difference method [18], the bilinear approach [19], A finite element method [20], the He's variational approach [21], the $\exp(-\varphi(\xi))$ -expansion technique [22], the unified method and its generalized form [23], the improved Bernoulli sub-equation function technique [24], the sine-cosine technique [25], the Bäcklund transformation scheme [26], the sub-equation method [27], the q -homotopy analysis transform method [28], the special computational method [29], etc.

Optical fiber communications are usually described by the perturbed NLS equation. In an optical fiber, light is contracted to a minor transverse section, so that even moderate optical powers lead to high optical intensities. This is particularly the case, if fibers are used to transmit short pulses. Moreover, the simplest and most common nonlinear effect in fibers is the Kerr effect. In addition, the phase delay in the fiber gets larger if the optical intensity increases. A medium, in which the light intensity passing through it depends on its refractive index, reveals the Kerr law nonlinearity. The NLS equation consists of temporal evolution term and the dispersion term. The delicate balance confirms the stable propagation and existence of such solitons. The perturbed NLS equation with Kerr law nonlinearity has been studied by a several researchers, namely, Zai-Yun et al. [30] investigated this equation by using the cosine function technique, Jacobi-elliptic function technique and found some analytic solutions including hyperbolic functions. In addition, Shehata [31] presented the modified (G'/G) -expansion technique for finding certain analytic solutions to the perturbed NLS equation. Bell, kink, and periodic soliton solutions of the perturbed NLS equation were obtained in [32]. By utilizing the direct algebraic technique, Eslami [33] derived some trigonometric function solutions to the perturbed NLS equation. The coupled NLS equation governs the evolution of spatial solitons in the photovoltaic photorefractive crystal studied by Dai and Wang [34]. Moreover, applying the modified auxiliary equation scheme, Mahak and Akram [35] describe the features of the perturbed NLS equation with Kerr law nonlinearity. They acquired singular and non-singular complex wave solutions together with bright soliton, stable periodic soliton and symmetric waves. In recent times, Al-Ghafri et al. [36] investigated the perturbed NLS equation with Kerr law nonlinearity and achieved W-shaped and other solitons appeared in optical nanofibers. Hosseini et al. [37] investigated the high-order nonlinear Schrödinger equation with non-Kerr law media for diverse laws of nonlinearities.

The model of nonlinear kinetics of radial dislocation in MTs plays a key role in describing the dynamical functional characteristics of microtubules. Generally, microtubules are filamentous intracellular structures that are responsible for numerous kinds of actions in all eukaryotic cells. Thus, it is important to understand the features of the microtubules as well as the composition, assembly, disassembly and how the functions are regulated by the cells. Moreover, Microtubules acts in nucleic and cell division, organization of intracellular structure, intracellular transport, as well as ciliary and flagellar motility. This model has been investigated by several researchers, viz., Zdravkovic et al. [38] describes the propagation of the solitary wave along the microtubules. Alam and Belgacem [39] applied the $\exp(-\varphi(\xi))$ expansion technique for obtaining the exponential and hyperbolic function solutions. They have also established kink and periodic solutions. Zdravkovic and Zekovic [40] executed the series expansion unknown function scheme for extracting nonlinear dynamics of microtubules. Zdravkovic [41] established the mechanical models of microtubules in which continuum and semi-discrete approximations were discussed. Continuum approximation provides bell-type or kink-type solitons, while semi-discrete

approximation computes the localized modulated waves moving along microtubules. Abdou [42] proposed the extended fractional sub-equation technique for fabricating the exact solutions of space-time fractional differential equations [43] appeared in nonlinear dynamics of microtubules. Justin et al. [44] studied chaotic vibration of microtubules in which chaos is one of the main cytoskeletal elements of eukaryotic cells. He also showed that the role of chaos in different biological information processing in microtubules. Owyed [45] et al. put in use three integral schemes, namely the generalized Kudryashov, Bernoulli sub-equation function and the improved $\exp(-\varphi(\xi))$ -expansion techniques for obtaining new optical soliton solutions of space-time fractional nonlinear dynamics of microtubules.

To obtain the analytic solutions of NLEEs Kudryashov [46] introduced a new technique recognized as Kudryashov approach. Akinyemi et al [47] investigated the dynamic solitons of the perturbed Biswas-Milovic equation of refractive index with Kudryashov's law using the first integral approach. The recently established generalized Kudryashov approach is compatible, realistic, and advantageous for extracting solitary wave solutions to NLEEs. This approach has been implemented to achieve stable and analytic solutions to the Klein-Fock-Gordon equation [48], the Riemann wave and the Novikov-Veselov equations [49], the Fokas-Lenells equation [50], the Konopelchenko-Dubrovsky and the Landau-Ginzburg-Higgs equations [51], the Korteweg-de-Vries equation [52], the telegraph equation [53], the Phi-four and the fisher equations [54], the Estevez-Mansfield-Clarkson (EMC) equation, the sine-Gordon equation [55], the Landau-Ginsburg-Higgs equation [56], etc.

To the optimal of our cognition and based on the analysis of the documents reachable in the literature, the perturbed NLS equation in the transmission of optical solitons occurring in optical fibers with Kerr law nonlinearity and the nonlinear model of the kinetics of radial dislocations in microtubules have not been investigated by using the generalized Kudryashov technique earlier. Thus, supported by the earlier studies, the aim of this article is to ascertain standard, realistic, and far-reaching compatible solutions to these equations through the generalized Kudryashov technique. We have also analyzed the physical characteristics and applicability of several obtained results to address the dynamical mechanisms of the wave equations under investigation.

The remainder of the article is structured as follows: The algorithms of the generalized Kudryashov approach are described in section 2. Section 3 extracts the solutions to the perturbed NLS and radial dislocations in microtubules (MTs) models. Section 4 is organized with the graphical representation and solution interpretations. The solutions are compared with those found in the literature in section 5, and in section 6, conclusions are drawn.

Algorithm of the generalized Kudryashov scheme

Consider a NLEE with space and time variable (x, t) as follows:

$$G(f, f_x, f_t, f_{xx}, f_{tt}, f_{xt}, \dots) = 0 \quad (1)$$

where $f(x, t)$ is unidentified function, G is the polynomial in $f(x, t)$ with partial derivatives including uppermost derivatives and nonlinear term. The contexts of the generalized Kudryashov scheme are narrated in the succeeding steps.

First step

It can be presumed the wave variables in the form $f(x, t) = f(\xi)$, $\xi = \kappa x \pm \omega t$ (here, κ and ω express the wave number and traveling wave speed respectively) is suitable to convert the equation (1) into the subsequent form of nonlinear equation:

$$H(f, f', f'') = 0 \quad (2)$$

Second step

Following the generalized Kudryashov approach, the solution of the nonlinear equation (2) is assumed in the succeeding form.

$$f(\xi) = \frac{\sum_{i=0}^N a_i q^i(\xi)}{\sum_{j=0}^M b_j q^j(\xi)} = \frac{a_0 + a_1 q(\xi) + a_2 q^2(\xi) + \dots + a_N q^N(\xi)}{b_0 + b_1 q(\xi) + b_2 q^2(\xi) + \dots + b_M q^M(\xi)} \tag{3}$$

where the coefficients $a_i (i = 0, 1, 2, \dots, N)$ and $b_j (j = 0, 1, 2, \dots, M)$ need to be evaluated afterwards with $a_N \neq 0$ and $b_M \neq 0$. The categorical solution of $q = q(\xi)$ will be pulling out from the nonlinear equation given below:

$$\frac{dq(\xi)}{d\xi} = q^2(\xi) - q(\xi). \tag{4}$$

Equation (4) possess a solution of the ensuing form.

$$q(\xi) = \frac{1}{1 + C \exp(\xi)}, \tag{5}$$

where C is an integrating parameter.

Third step

The homogeneous balance technique is used to determine the positive integrals N and M come out in solution (3).

Fourth step

Inserting the solution (3) into equation (2) with the aid of equation (4), a polynomial in $q(\xi)$ can be obtained. Then the similar index of $q(\xi)$ are equating to zero delivers an algebraic system of equation. Solving these equations by using Maple it can be achieved the values of the desired constants a_i, b_j and ω which will be used to attain the solution of equation (2).

Extraction of solutions

This segment describes the effectiveness of the generalized Kudryashov scheme to pursue scores of soliton solutions of two NLEEs, namely, the perturbed NLS equation with Kerr law nonlinearity and the nonlinear dynamics of the radial dislocation in MTs.

Perturbed NLS equation with Kerr law nonlinearity

Considering the perturbed NLS equation with Kerr law nonlinearity [30]:

$$iu_t + u_{xx} + \alpha |u|^2 + i[\gamma_1 u_{xxx} + \gamma_2 |u|^2 u_x + \gamma_3 (|u|^2)_x u] = 0. \tag{6}$$

wherein γ_1 is a third order dispersion restraint and γ_2, γ_3 are steeping cohort. Equation (6) represents the extension of optical solutions in nonlinear optical fibers with Kerr law nonlinearity [32]. We assume the subsequent wave variable for equation (6).

$$u(x, t) = v(\xi) \exp(i\psi)$$

where

$$\xi = \beta x + ct, \psi = kx - \omega t \tag{7}$$

where c is the speed of wave propagation. Equation (6) is converted into a nonlinear equation by means of the wave transformation variable (7), and splitting the real and imaginary parts, we find the following couple of equations.

$$\gamma_1 \beta^3 v + (\gamma_2 \beta + 2\gamma_3) + (c + 2k\beta - 3\gamma_1 k^2 \beta) v = 0. \tag{8}$$

$$\beta^2 (1 - 3\gamma_1 k) v'' + (\omega - k^2 + \gamma_1 k^3) v + (\alpha - \gamma_2 k) v^3 = 0. \tag{9}$$

Integrating (8) by keeping constant of integration to be zero, we find.

$$\gamma_1 \beta^3 v'' + \{c - \beta k(3\gamma_1 k - 2)\} v + \frac{1}{3} \beta (\gamma_2 + 2\gamma_3) v^3 = 0. \tag{10}$$

For $c = \beta k(3\gamma_1 k - 2)$, $\omega = k^2(1 - \gamma_1 k)$, $k = (\gamma_2 + 2\gamma_3 - 3\alpha\gamma_1) / 6\gamma_1\gamma_3$ and $\beta = (3\alpha\gamma_1 - 2\gamma_2) / 2\gamma_1\gamma_3$, Eqs. (9) and (10) are identical. Therefore, it is sufficient to solve either of these two equations. We will investigate Eq. (10), therefore, assuming $R = \beta^3 \gamma_1$, $S = \beta k(3\gamma_1 k - 2)$ and $T = \frac{1}{3} \beta (\gamma_2 + 2\gamma_3)$, Eq. (10) can be written in the subsequent form:

$$R v'' + (c - S)v + Tv^3 = 0. \tag{11}$$

Eq. (11) and the Eq. (1) in Ref. [57] are analogous. Equation (1) in Ref. [57] was solved directly and tanh, rational and exponential type solutions have been obtained. Alternatively, in this article, the Eq. (11) has been investigated by the generalized Kudryashov method. In requirement of the Kudryashov approach, we consider the homogeneous balance between v'' and v^3 in equation (11) and it is established the relation $N = M + 1$ which delivers $N = 2$ for $M = 1$. Therefore, solution (3) is simplified in the following form.

$$v(\xi) = \frac{a_0 + a_1 q + a_2 q^2}{b_0 + b_1 q}, \tag{12}$$

wherein $a_2 \neq 0$ and the constants a_0, a_1, a_2, b_0 and b_1 are to be determined. Introducing the solution (12) along with equation (4) into equation (11) and equating the comparable exponent of $q(\xi)$ to zero, subsequent algebraic set of equations can be attained.

$$Ta_0^3 + ca_0b_0^2 - Sa_0b_0^2 = 0.$$

$$Ra_1b_0^2 + ca_1b_0^2 - Sa_1b_0^2 + 3Ta_0^2a_1 - Rb_1a_0b_0 + 2ca_0b_1b_0 - 2Sa_0b_1b_0 = 0.$$

$$-3Ra_1b_0^2 + Rb_1^2a_0 + ca_0b_1^2 + ca_2b_0^2 - Sa_0b_1^2 - Sa_2b_0^2 + 3Ta_0^2a_2 + 3Ta_0a_1^2 + 4Ra_2b_0^2 + 3Rb_1a_0b_0 - Ra_1b_0b_1 + 2ca_1b_1b_0 - 2sa_1b_1b_0 = 0.$$

$$Ta_1^3 + ca_1b_1^2 - Sa_1b_1^2 + 2Ra_1b_0^2 - 10Ra_2b_0^2 - Rb_1^2a_0 + Ra_1b_0b_1 = 0.$$

$$-2Rb_1a_0b_0 + 3Ra_2b_0b_1 + 2ca_2b_1b_0 - 2Sa_2b_1b_0 + 6Ta_0a_1a_2 = 0.$$

$$ca_2b_1^2 - Sa_2b_1^2 + 3Ta_0a_2^2 + 3Ta_1^2a_2 + 6Ra_2b_0^2 + Rb_1^2a_2 - 9Ra_2b_0b_1 = 0.$$

$$3Ta_1a_2^2 - 3Rb_1^2a_2 + 6Ra_2b_0b_1 = 0.$$

$$Ta_2^3 + 2Rb_1^2a_2 = 0.$$

Using computer algebra system Maple, we analyze the above system of equations and obtain the following group of values and the respective solutions:

Cohort 1

$$c = \frac{1}{2}R + S, a_0 = 0, a_1 = \frac{1}{2} \frac{\sqrt{-2TR}b_1}{T}, a_2 = \frac{2Rb_1}{\sqrt{-2TR}}, b_0 = 0, b_1 = b_1.$$

Introducing these values into the solution (12) with the help of equation (5), we obtain the following exponential function solution

$$v(\xi) = -\frac{R}{\sqrt{-2TR}} \left(\frac{-1 + A \exp(\xi)}{1 + A \exp(\xi)} \right). \tag{13}$$

This solution can be transformed into the hyperbolic function

$$v(\xi) = -\frac{R}{\sqrt{-2TR}} \left(\frac{(A - 1) \cosh(\xi/2) + (A + 1) \sinh(\xi/2)}{(A + 1) \cosh(\xi/2) + (A - 1) \sinh(\xi/2)} \right). \tag{14}$$

Connecting the solution together with time-space variables, we

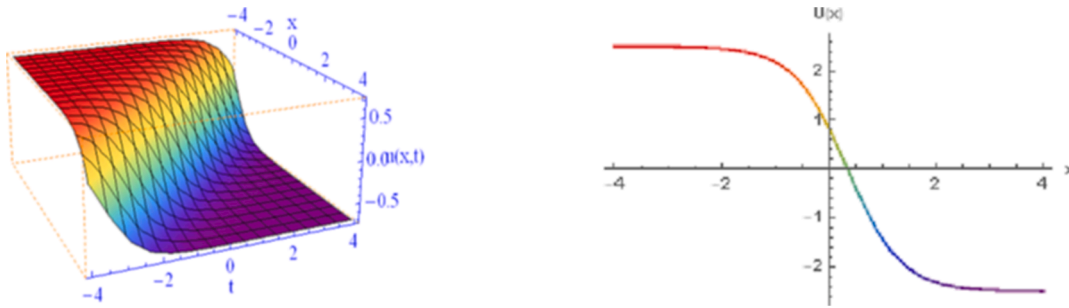


Fig. 1. 3D and 2D plots of solution (16) corresponding to $c = -2$ and other definite values $R = T = \beta = -2$.

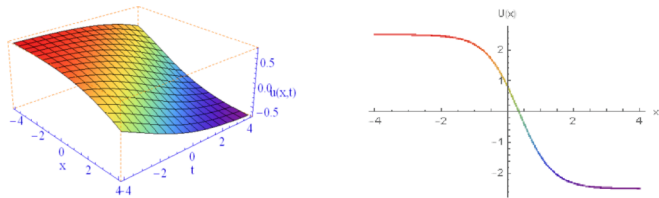


Fig. 2. 3D and 2D plots of solution (16) corresponding to $c = -0.54$ and other definite values $R = T = -2, \beta = -0.48$.

attain the ensuing rational function solution

$$u(x, t) = -\frac{R}{\sqrt{-2TR}} \left(\frac{(A-1)\cosh\left(\frac{\beta x + ct}{2}\right) + (A+1)\sinh\left(\frac{\beta x + ct}{2}\right)}{(A+1)\cosh\left(\frac{\beta x + ct}{2}\right) + (A-1)\sinh\left(\frac{\beta x + ct}{2}\right)} \right) \exp(i(kx - \omega t)). \tag{15}$$

Since A is an integrating constant, we might designate its value independently. Choosing $A = 2$, solution (15) turns into the form

$$u(x, t) = -\frac{R}{\sqrt{-2TR}} \left(\frac{\cosh\left(\frac{\beta x + ct}{2}\right) + 3\sinh\left(\frac{\beta x + ct}{2}\right)}{3\cosh\left(\frac{\beta x + ct}{2}\right) + \sinh\left(\frac{\beta x + ct}{2}\right)} \right) \exp(i(kx - \omega t)). \tag{16}$$

Again, choosing $A = 4$, solution (15) turns into the form

$$u(x, t) = -\frac{R}{\sqrt{-2TR}} \left(\frac{3\cosh\left(\frac{\beta x + ct}{2}\right) + 5\sinh\left(\frac{\beta x + ct}{2}\right)}{5\cosh\left(\frac{\beta x + ct}{2}\right) + 3\sinh\left(\frac{\beta x + ct}{2}\right)} \right) \exp(i(kx - \omega t)). \tag{17}$$

On the other hand, choosing $A = 1$, solution (15) becomes

$$u(x, t) = -\frac{R}{\sqrt{-2TR}} \tanh\left(\frac{\beta x + ct}{2}\right) \exp(i(kx - \omega t)). \tag{18}$$

Furthermore, choosing $A = -1$, solution (15) becomes

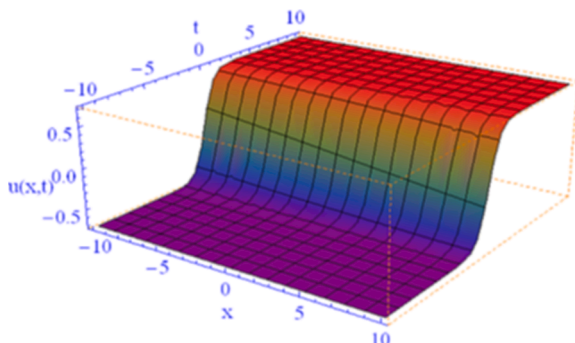


Fig. 3. 3D and 2D profiles of solution (18) for $c = -0.06$ and other fixed values $R = T = -2, \beta = 2$.

$$u(x, t) = -\frac{R}{\sqrt{-2TR}} \coth\left(\frac{\beta x + ct}{2}\right) \exp(i(kx - \omega t)). \tag{19}$$

In the similar way, varying the integral constant A results other analytic solutions. However, for the sake of conciseness, these solutions are not included in this section.

Cohort 2

$$c = -R + S, a_0 = 0, a_1 = \frac{2\sqrt{-2TR}b_0}{T}, a_2 = -\frac{2\sqrt{-2TR}b_0}{T}, b_0 = b_0, b_1 = -2b_0$$

With the help of (5), we obtain the following solution by inserting the values stated above in the solution formula (12):

$$v(\xi) = 2\sqrt{\frac{-2R}{T}} \frac{A}{A^2 \exp(\xi) - \exp(-\xi)}. \tag{20}$$

In hyperbolic form, it can be expressed in terms of space and time coordinates as

$$v(x, t) = 2\sqrt{\frac{-2R}{T}} \frac{A}{(A^2 - 1)\cosh(\beta x + ct) + (A^2 + 1)\sinh(\beta x + ct)}. \tag{21}$$

Connecting the wave variable in equation (7) formulates the new general solution structure

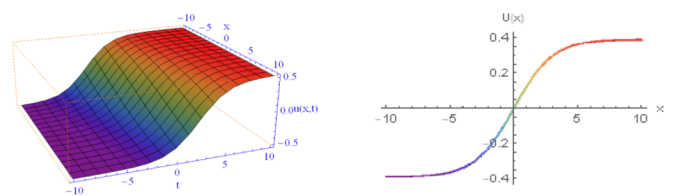


Fig. 4. 3D and 2D profiles of solution (18) for the wave speed $c = 0.15$ and other fixed values $\beta = -0.67, R = 1.09, T = 2$.

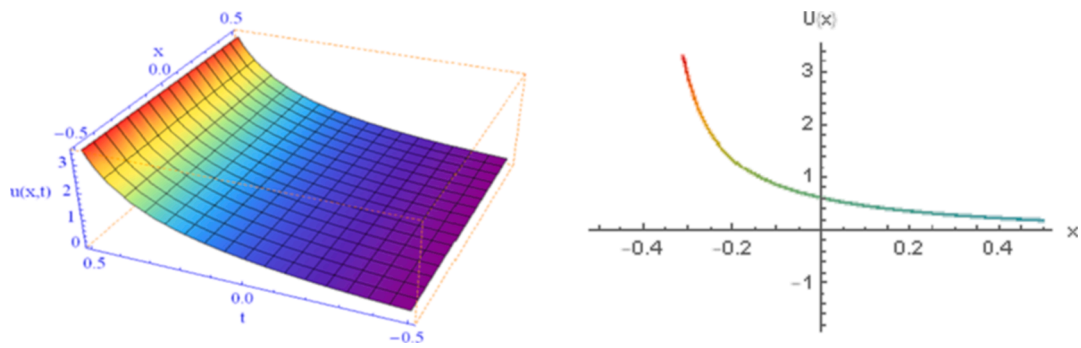


Fig. 5. 3D and 2D envelopes of solution (22) for $c = -0.01$ and other values $A = -0.25, \beta = 1.97, R = T = -2$.

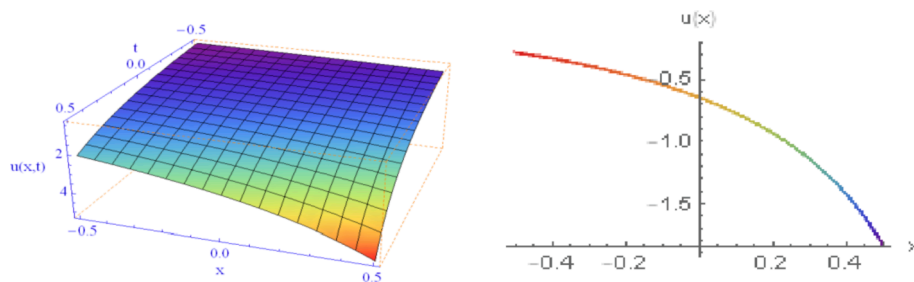


Fig. 6. 3D and 2D envelopes of solution (22) for the wave speed $c = 0.54$ and other values $A = -0.23, \beta = 1.51, R = -2, T = -0.69$.

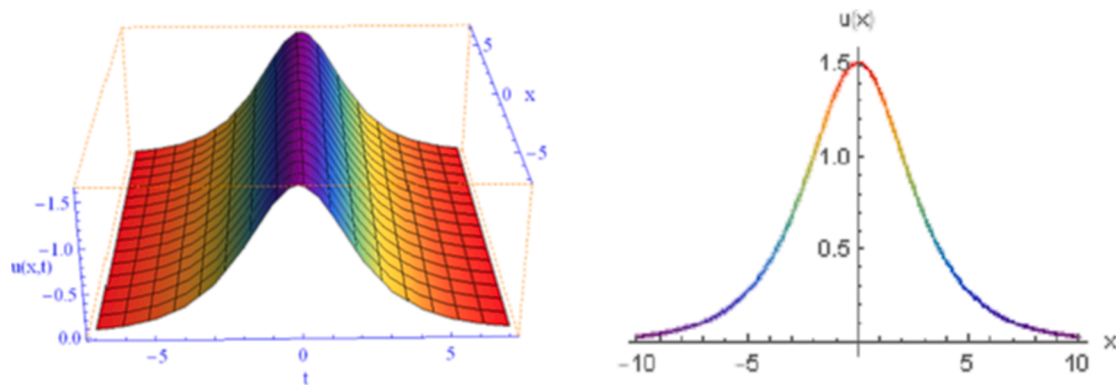


Fig. 7. 3D and 2D plots of solution (26) regarding $c = -1.24$ and other values of $\beta = 0.03, R = -1.18, T = -0.90$.

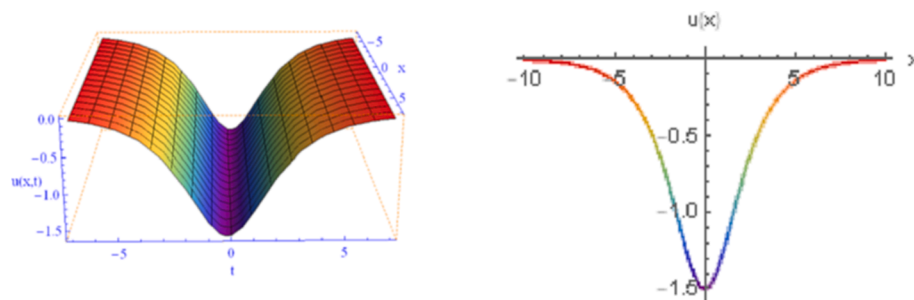


Fig. 8. 3D and 2D plots of solution (26) regarding the wave speed $c = 1.21$ and other values of $\beta = 0.03, R = -1.18, T = -0.90$.

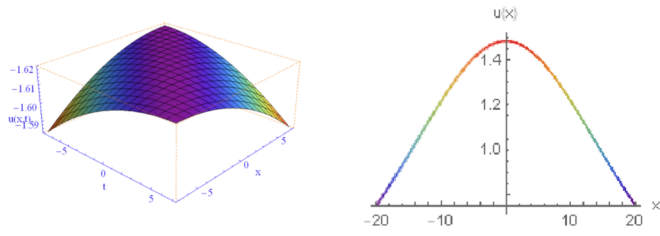


Fig. 9. 3D and 2D contours of solution (26) for the wave speed $c = 0.03$ and other values of $T = -0.90, \beta = 0.03, R = -1.18$.

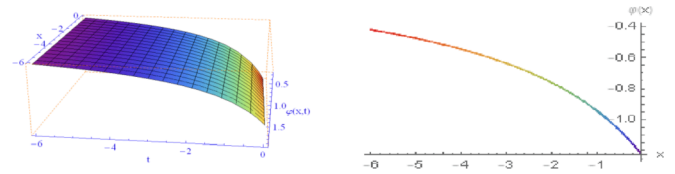


Fig. 14. 3D and 2D profiles of solution (40) corresponding to the wave speed $\omega = 0.15$ and other values of $A = 1.26, \kappa = -0.01$.

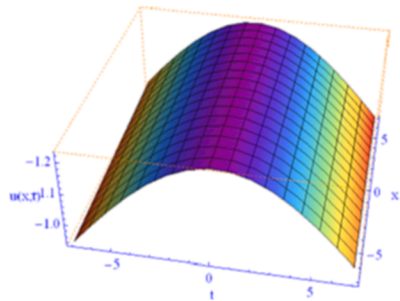


Fig. 10. 3D and 2D contours of solution (26) for $c = -0.21$ and other values of $\beta = -0.01, R = -0.73, T = -0.97$.

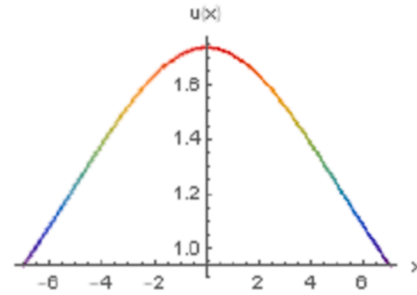


Fig. 11. 3D and 2D structures of solution (29) due to $c = -0.01$ and other values of $A = -0.12, \beta = -0.54, R = -0.88, T = -0.90$.

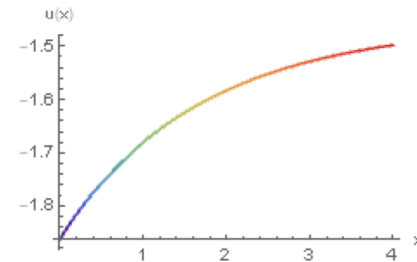
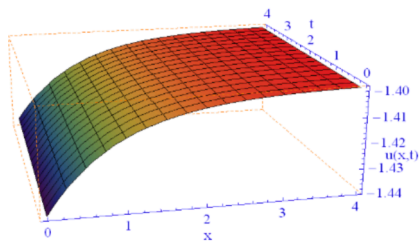


Fig. 12. 3D and 2D structures of solution (29) due to the wave velocity $c = 0.01$ and other values of $A = -0.12, \beta = 1.51, R = -0.80, T = -0.90$.

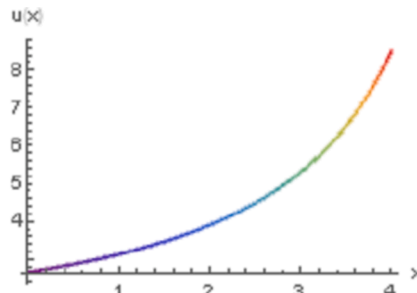
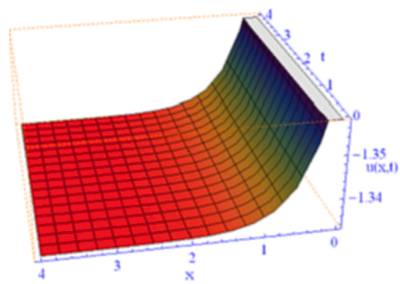


Fig. 13. 3D and 2D profiles of solution (40) corresponding to the wave speed $\omega = 0.39$ and other values of $A = 1.26, \kappa = -0.01$.

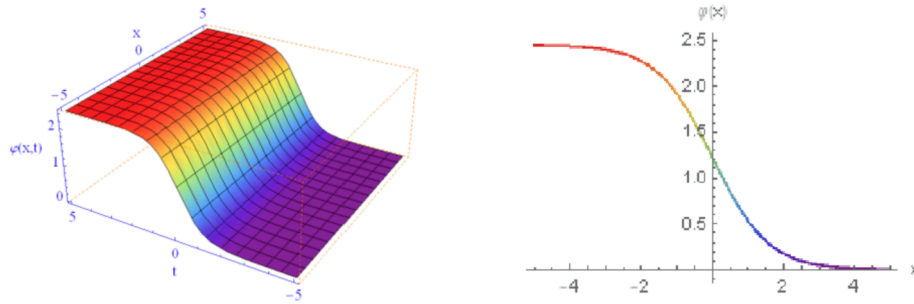


Fig. 15. 3D and 2D contours of solution (48) regarding the wave speed $\omega = 2$ and other constant $\kappa = 0.03$.

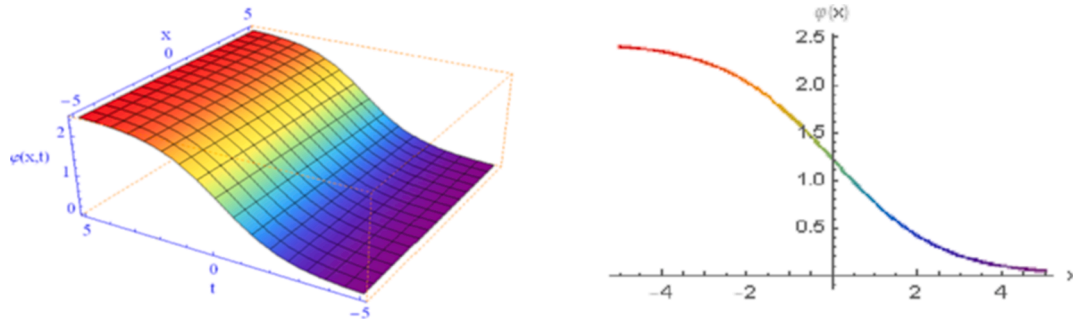


Fig. 16. 3D and 2D contours of solution (50) regarding the wave speed $\omega = 0.92$ and other constant $\kappa = 0.03$.

$$u(x, t) = 2\sqrt{\frac{-2R}{T}} \frac{A}{(A^2 - 1)\cosh(\beta x + ct) + (A^2 + 1)\sinh(\beta x + ct)} \exp(i(kx - \omega t)). \quad (22)$$

Since A is an integrating constant, one might accept its value extensively. For the value $A = 2$, we derive the soliton solution in terms of the hyperbolic function

$$u(x, t) = 2\sqrt{\frac{-2R}{T}} \frac{2}{3\cosh(\beta x + ct) + 5\sinh(\beta x + ct)} \exp(i(kx - \omega t)). \quad (23)$$

For the value $A = -4$, we attain the following soliton solution in terms of hyperbolic form

$$u(x, t) = 2\sqrt{\frac{-2R}{T}} \frac{-4}{15\cosh(\beta x + ct) + 17\sinh(\beta x + ct)} \exp(i(kx - \omega t)). \quad (24)$$

For $A = 1$, we obtain a solution of the form

$$u(x, t) = \sqrt{\frac{-2R}{T}} \operatorname{csch}(\beta x + ct) \exp(i(kx - \omega t)). \quad (25)$$

Again, for $A = i$, the solution (22) turns into the form given below

$$u(x, t) = \sqrt{\frac{2R}{T}} \operatorname{sech}(\beta x + ct) \exp(i(kx - \omega t)). \quad (26)$$

Similarly, for different values of the integral constant A , different types of analytic solutions emerge. These solutions, however, are not recorded in this part for the sake of simplicity.

Cohort 3

$$c = 2R + S, a_0 = -\frac{Rb_1}{\sqrt{-2TR}}, a_1 = \frac{2Rb_1}{\sqrt{-2TR}}, a_2 = \frac{\sqrt{-2TR}b_1}{T}, b_0 = -\frac{1}{2}b_1, b_1 = b_1.$$

Assigning the preceding values into the solution (12), by taking equation (5) into account, we obtain the following soliton solution

$$v(\xi) = \sqrt{\frac{2R}{-T}} \frac{A^2 \exp(\xi) + \exp(-\xi)}{A^2 \exp(\xi) - \exp(-\xi)}. \quad (27)$$

This solution can be transformed into the subsequent hyperbolic function solution

$$v(\xi) = \sqrt{\frac{2R}{-T}} \frac{(A^2 - 1)\sinh(\xi) + (A^2 + 1)\cosh(\xi)}{(A^2 + 1)\sinh(\xi) + (A^2 - 1)\cosh(\xi)}. \quad (28)$$

We determine the resulting rational function solution relating to the solution (28) with the space and time variables

$$u(x, t) = \sqrt{\frac{2R}{-T}} \frac{(A^2 - 1)\sinh(\beta x + ct) + (A^2 + 1)\cosh(\beta x + ct)}{(A^2 + 1)\sinh(\beta x + ct) + (A^2 - 1)\cosh(\beta x + ct)} \exp(i(kx - \omega t)). \quad (29)$$

Since A is a subjective constant, we might accept its value intuitively. Thus, for $A = \pm\sqrt{2}$, we attain the next soliton solution

$$u(x, t) = \sqrt{\frac{2R}{-T}} \frac{3\sinh(\beta x + ct) + 5\cosh(\beta x + ct)}{5\sinh(\beta x + ct) + 3\cosh(\beta x + ct)} \exp(i(kx - \omega t)). \quad (30)$$

Moreover, for the value $A = \pm\sqrt{6}$, we ascertain the under mentioned soliton solution

$$u(x, t) = \sqrt{\frac{2R}{-T}} \frac{35\sinh(\beta x + ct) + 37\cosh(\beta x + ct)}{37\sinh(\beta x + ct) + 35\cosh(\beta x + ct)} \exp(i(kx - \omega t)). \quad (31)$$

For $A = \pm i$, we develop the tanh function solution of the form

$$u(x, t) = \sqrt{\frac{2R}{-T}} \tanh(\beta x + ct) \exp(i(kx - \omega t)). \quad (32)$$

Many more solutions can be obtained by putting distinct values of the integrating constant A in each group. Due to simplicity, we did not report those solutions herein.

The obtained soliton solutions have substantial applications in different fields of science and engineering, such as the propagation of light in optical fiber and planar waveguides including self-phase modulation, four-wave mixing, ultra-short pulses, optical solitons,

Table 1
Comparison of the results of the perturbed NLS equation [58].

The results accomplished in this article	
The results of Moosaei et al. [58]	
The solution (22) is	
$u(x, t) = - \left\{ \sqrt{\frac{6A_0\gamma_1}{\sqrt{-6\gamma_1(\gamma_2 + 2\gamma_3)}}} \tan \left[\frac{A_0 \sqrt{-6\gamma_1(\gamma_2 + 2\gamma_3)}}{6\gamma_1} \times (x - (2K - 3\gamma_1 K^2 + \frac{A_0}{3} \sqrt{-6\gamma_1(\gamma_2 + 2\gamma_3)})t + \xi_0) \right] \right\} e^{i(\kappa x - \omega t)}$	$u(x, t) = - \frac{R}{\sqrt{-2TR}} \left(\frac{3 \cosh\left(\frac{\beta x + ct}{2}\right) + 5 \sinh\left(\frac{\beta x + ct}{2}\right)}{5 \cosh\left(\frac{\beta x + ct}{2}\right) + 3 \sinh\left(\frac{\beta x + ct}{2}\right)} \right) \exp(i(\kappa x - \omega t)).$
The solution (24) is	
$u(x, t) = - \left\{ \sqrt{\frac{6A_0\gamma_1}{\sqrt{-6\gamma_1(\gamma_2 + 2\gamma_3)}}} \tanh \left[\frac{A_0 \sqrt{-6\gamma_1(\gamma_2 + 2\gamma_3)}}{6\gamma_1} \times (x - (2K - 3\gamma_1 K^2 - \frac{A_0}{3} \sqrt{-6\gamma_1(\gamma_2 + 2\gamma_3)})t + \xi_0) \right] \right\} e^{i(\kappa x - \omega t)}$	$u(x, t) = \frac{R}{\sqrt{-2TR}} \coth\left(\frac{\beta x + ct}{2}\right) \exp(i(\kappa x - \omega t)).$
The solution (33) is	
$u(x, t) = \pm \left\{ \sqrt{\frac{3(-2K + 3\gamma_1 K^2 + c)}{(\gamma_2 + 2\gamma_3)}} \times \tanh \left[\frac{(2K - 3\gamma_1 K^2 - c)}{2\gamma_1} (x - ct + \xi_0) \right] \right\} e^{i(\kappa x - \omega t)}$	$u(x, t) = \frac{2R}{T} \operatorname{sech}\left(\frac{\beta x + ct}{2}\right) \exp(i(\kappa x - \omega t)).$
$u(x, t) = \pm \left\{ \sqrt{\frac{3(-2K + 3\gamma_1 K^2 - c)}{(\gamma_2 + 2\gamma_3)}} \times \tanh \left[\frac{(2K - 3\gamma_1 K^2 - c)}{2\gamma_1} (x - ct + \xi_0) \right] \right\} e^{i(\kappa x - \omega t)}$	$u(x, t) = \frac{-2R}{T} \operatorname{csch}\left(\frac{\beta x + ct}{2}\right) \exp(i(\kappa x - \omega t)).$
$u(x, t) = \pm \left\{ \sqrt{\frac{3(-2K + 3\gamma_1 K^2 - c)}{(\gamma_2 + 2\gamma_3)}} \times \tanh \left[\frac{(2K - 3\gamma_1 K^2 - c)}{2\gamma_1} (x - ct + \xi_0) \right] \right\} e^{i(\kappa x - \omega t)}$	$u(x, t) = \frac{2R}{T} \tanh(\beta x + ct) \exp(i(\kappa x - \omega t)).$

Table 2
Comparison of the determined results with Zdravkovic' et al. [60].

Zdravkovic' et al. [60] solutions	Solutions established in this article
<p>The result (16) is</p> $\varphi(x, t) = \frac{K}{2} \left(1 + \tanh\left(\frac{3(\kappa x - \omega t)}{4\rho}\right) \right).$	<p>The results (49), (50) and (51) are</p> $\varphi(x, t) = \pm \sqrt{6} \frac{\cosh(\kappa x - \omega t) - \sinh(\kappa x - \omega t)}{11 \cosh(\kappa x - \omega t) + 13 \sinh(\kappa x - \omega t)}$ $\varphi(x, t) = \mp \frac{\sqrt{6}}{2} \left(1 - \tanh\left(\frac{\kappa x - \omega t}{2}\right) \right).$ $\varphi(x, t) = \mp \frac{\sqrt{6}}{2} \left(1 - \coth\left(\frac{\kappa x - \omega t}{2}\right) \right).$
<p>The result (24) is</p> $i \frac{K'}{2} \left(1 + \tanh\left(\frac{3(\kappa x - \omega t)}{4\rho}\right) \right).$	<p>The results (57) and (58) are</p> $\varphi(x, t) = -4\sqrt{6} \left(\frac{\cosh\left(\frac{\kappa x - \omega t}{2}\right) + \sinh\left(\frac{\kappa x - \omega t}{2}\right)}{-3 \cosh\left(\frac{\kappa x - \omega t}{2}\right) - 5 \sinh\left(\frac{\kappa x - \omega t}{2}\right)} \right).$ $\varphi(x, t) = \frac{\sqrt{6}}{2} \left(1 + \tanh\left(\frac{\kappa x - \omega t}{2}\right) \right).$

stimulated Raman scattering etc.

Nonlinear dynamics of the radial dislocation in MTs

The nonlinear dynamics of the radial dislocations in MTs can be expressed in the following form [38]:

$$I \frac{\partial^2 \varphi}{\partial t^2} - kl^2 \frac{\partial^2 \varphi}{\partial x^2} + pE\varphi - \frac{pE}{6} \varphi^3 + \gamma \frac{\partial \varphi}{\partial t} = 0, \tag{33}$$

where $\varphi(x, t)$ represents the angular displacement of the whole dimer, l implies the MTs length, p signifies the intrinsic electric field magnitude, k denotes the bonding interaction of inter dimer within the same protofilaments (PFs), I represents the coefficient of viscosity.

To remodel (33) into nonlinear equation, we use the following unified coordinate

$$\varphi(x, t) = \varphi(\xi)$$

where

$$\xi = \kappa x - \omega t, \tag{34}$$

where in κ and ω defines the nonzero constants representing the wave number and frequency respectively. Thus, equation (33) converts to

$$(I\omega^2 - kl^2 \kappa^2) \varphi'' - \gamma \omega \varphi' + pE\varphi - \frac{pE}{6} \varphi^3 = 0. \tag{35}$$

The following potential transformation

$$\varphi(\xi) = \sqrt{6}u(\xi), \tag{36}$$

converts the equation (35) into the ensuing form

$$\frac{(I\omega^2 - kl^2 \kappa^2)}{pE} u'' - \frac{\omega \gamma}{pE} u' + u - u^3 = 0. \tag{37}$$

According to the principle of generalized Kudryashov scheme, balancing u'' and u^3 in equation (37), we obtain $N = 2$ for $M = 1$ from the balancing relation $N = M + 1$. Thus, the solution (3) can be stated in the ensuing form

$$u(\xi) = \frac{a_0 + a_1 q + a_2 q^2}{b_0 + b_1 q}, \tag{38}$$

where a_2 and b_1 are non-zero constants. Embedding the solution (38) into (37) and setting the conforming power of $q(\xi)$ to zero, it is obtained the following set of algebraic equations.

$$pEa_0^3 - pEa_0b_0^2 = 0$$

$$-kl^2 \kappa^2 b_1 a_0 b_0 + I\omega^2 b_1 a_0 b_0 + \gamma \omega b_1 a_0 b_0 - 2pEb_1 a_0 b_0 = 0$$

$$\begin{aligned}
 &3kl^2\kappa^2b_1a_0b_0 + kl^2\kappa^2b_1^2a_0 - \gamma\omega b_1a_0b_0 - 3I\omega^2b_1a_0b_0 + 4kl^2\kappa^2a_2b_0^2 - I\omega^2b_1^2a_0 \\
 &+ \gamma\omega b_1^2a_0 - pEb_1^2a_0 - pEa_2b_0^2 - 4I\omega^2a_2b_0^2 - 2\gamma\omega a_2b_0^2 + 3pEa_0^2a_2 = 0 \\
 &3kl^2\kappa^2a_2b_0b_1 - 2kl^2\kappa^2b_1a_0 + I\omega^2b_1^2a_0 - \gamma Ib_1^2a_0 + 10I\omega^2a_2b_0^2 + 2\gamma\omega ab_0^2 - kl^2\kappa^2b_1^2a_0 \\
 &- 3I\omega^2a_2b_0b_1 - 10kl^2\kappa^2a_2b_0^2 + 2I\omega^2b_1a_0b_0 - 3\gamma\omega a_2b_0b_1 - 2pEa_2b_0b_1 = 0 \\
 &- 9kl^2\kappa^2a_2b_0b_1 + kl^2\kappa^2a_2b_1^2 + 9I\omega^2a_2b_0b_1 + 6kl^2\kappa^2a_2b_0^2 + 3\gamma\omega a_2b_0b_1 \\
 &- \gamma\omega a_2b_1^2 - pEa_2b_1^2 - 6I\omega^2a_2b_0^2 + 3pEa_0^2a_2 - I\omega^2a_2b_1^2 = 0 \\
 &6kl^2\kappa^2a_2b_0b_1 - 3kl^2\kappa^2a_2b_1^2 - 6I\omega^2a_2b_0b_1 + \gamma\omega a_2b_1^2 + 3I\omega^2a_2b_1^2 = 0 \\
 &- 2I\omega^2a_2b_1^2 + pEa_2^3 + 2kl^2\kappa^2a_2b_1^2 = 0
 \end{aligned}$$

The aforementioned set of equations has been interpreted using Maple, and found the subsequent solutions:

Cohort 1

$$\begin{aligned}
 \kappa &= \pm \frac{\sqrt{kEp(9EI p - 2\gamma^2)}}{2k\gamma l}, \omega = -\frac{3}{2} \frac{pE}{\gamma}, a_0 = 0, a_1 = 0, a_2 = \pm b_1, b_0 \\
 &= 0, b_1 = b_1.
 \end{aligned}$$

Using the values of the parameters accumulated in cohort 1 into solution (38) and connected to the solution (36) give an exponential function solution in the subsequent form

$$\varphi(\xi) = \pm \frac{\sqrt{6}}{1 + A \exp(\xi)} \tag{39}$$

The definite structure of the waves is necessary to describe the solutions in a realistic way. Since the hyperbolic function provides good structure, we will convert the exponential function into hyperbolic function. Therefore, the hyperbolic identity develops the above solution into the ensuing form

$$\varphi(x, t) = \pm \frac{\sqrt{6}}{1 + A(\cosh(\kappa x - \omega t) + \sinh(\kappa x - \omega t))} \tag{40}$$

For integral constant $A = \pm 3$, the solution (40) becomes

$$\varphi(x, t) = \pm \frac{\sqrt{6}}{1 \pm 3(\cosh(\kappa x - \omega t) + \sinh(\kappa x - \omega t))} \tag{41}$$

Furthermore, the value of $A = \pm 7$ represents an explicit soliton

$$\varphi(x, t) = \pm \frac{\sqrt{6}}{1 \pm 7(\cosh(\kappa x - \omega t) + \sinh(\kappa x - \omega t))} \tag{42}$$

But, for $A = 1$, from (39) we obtain the standard kink soliton solution

$$\varphi(x, t) = \pm \frac{\sqrt{6}}{2} \left(1 - \tanh\left(\frac{\kappa x - \omega t}{2}\right) \right), \tag{43}$$

where $\kappa = \pm \frac{\sqrt{kEp(9EI p - 2\gamma^2)}}{2k\gamma l}$ and $\omega = -\frac{3}{2} \frac{pE}{\gamma}$. For alternative values of the integral constant A , there can be established other exact solutions. These solutions, however, are not determined in this section due to length constraints.

Cohort 2

$$\begin{aligned}
 \kappa &= \pm \frac{\sqrt{kEp(9EI p - 2\gamma^2)}}{4k\gamma l}, \omega = -\frac{3}{4} \frac{pE}{\gamma}, a_0 = 0, a_1 = 0, a_2 = \pm \frac{1}{2} b_1, b_0 \\
 &= -\frac{1}{2} b_1, b_1 = b_1.
 \end{aligned}$$

Inserting these values into the solution (38) and along with (36), we

derive the succeeding form of solution

$$\varphi(\xi) = \pm \frac{\sqrt{6}}{-1 + A^2 \exp(2\xi)} \tag{44}$$

The hyperbolic identity develops the above solution into the ensuing form

$$\varphi(x, t) = \pm \sqrt{6} \frac{\cosh(\kappa x - \omega t) - \sinh(\kappa x - \omega t)}{(A^2 - 1)\cosh(\kappa x - \omega t) + (A^2 + 1)\sinh(\kappa x - \omega t)} \tag{45}$$

Since the above solution has an integrating constant A , we might opt its value subjectively. Therefore, solution (45) turns into the hyperbolic (sinh, cosh) function for $A = \pm\sqrt{2}$.

$$\varphi(x, t) = \pm \sqrt{6} \frac{\cosh(\kappa x - \omega t) - \sinh(\kappa x - \omega t)}{3\cosh(\kappa x - \omega t) + 5\sinh(\kappa x - \omega t)} \tag{46}$$

Similarly, for $A = \pm 2\sqrt{3}$, from solution (45), we attain

$$\varphi(x, t) = \pm \sqrt{6} \frac{\cosh(\kappa x - \omega t) - \sinh(\kappa x - \omega t)}{11\cosh(\kappa x - \omega t) + 13\sinh(\kappa x - \omega t)} \tag{47}$$

But, for $A = \pm i$, we ascertain kink shape soliton from (46) as follows:

$$\varphi(x, t) = \pm \frac{\sqrt{6}}{2} \left(1 - \tanh\left(\frac{\kappa x - \omega t}{2}\right) \right). \tag{48}$$

Furthermore, for $A = 1$, from solution (46), we found the singular kink soliton given as:

$$\varphi(x, t) = \pm \frac{\sqrt{6}}{2} \left(1 - \coth\left(\frac{\kappa x - \omega t}{2}\right) \right) \tag{49}$$

where $\kappa = \pm \frac{\sqrt{kEp(9EI p - 2\gamma^2)}}{4k\gamma l}$ and $\omega = -\frac{3}{4} \frac{pE}{\gamma}$. For other values of the elementary constant A , there can obtain further exact solutions. These solutions, however, are not documented in this section due to length limitation.

Cohort 3

$$\begin{aligned}
 \kappa &= \pm \frac{\sqrt{kEp(9EI p - 2\gamma^2)}}{2k\gamma l}, \omega = \frac{3}{2} \frac{pE}{\gamma}, a_0 = b_1, a_1 = 0, a_2 = -b_1, b_0 \\
 &= b_1, b_1 = b_1.
 \end{aligned}$$

Placing the values arranged in cohort 3 into solution (38) and considering of solution (36) formulates an explicit solution in terms of exponential function.

$$\varphi(\xi) = \frac{\sqrt{6}A \exp(\xi/2)}{A \exp(\xi/2) + \exp(-\xi/2)} \tag{50}$$

The hyperbolic identity develops the above solution into the ensuing form

$$\varphi(x, t) = \sqrt{6}A \left(\frac{\cosh\left(\frac{\kappa x - \omega t}{2}\right) + \sinh\left(\frac{\kappa x - \omega t}{2}\right)}{(A + 1)\cosh\left(\frac{\kappa x - \omega t}{2}\right) + (A - 1)\sinh\left(\frac{\kappa x - \omega t}{2}\right)} \right). \tag{51}$$

Since the above solution has an integrating constant A , one might select its value definitely. Therefore, solution (51) develops to the rational function solution for $A = 2$.

$$\varphi(x, t) = 2\sqrt{6} \left(\frac{\cosh\left(\frac{\kappa x - \omega t}{2}\right) + \sinh\left(\frac{\kappa x - \omega t}{2}\right)}{3\cosh\left(\frac{\kappa x - \omega t}{2}\right) + \sinh\left(\frac{\kappa x - \omega t}{2}\right)} \right). \tag{52}$$

If we put $A = \pm 4$, solution (51) is noted as

$$\varphi(x, t) = 4\sqrt{6} \left(\frac{\cosh\left(\frac{\kappa x - \omega t}{2}\right) + \sinh\left(\frac{\kappa x - \omega t}{2}\right)}{5\cosh\left(\frac{\kappa x - \omega t}{2}\right) + 3\sinh\left(\frac{\kappa x - \omega t}{2}\right)} \right). \tag{53}$$

But, if we select $A = 1$, solution (53) takes the tanh function solution

$$\varphi(x, t) = \frac{\sqrt{6}}{2} \left(1 + \tanh\left(\frac{\kappa x - \omega t}{2}\right) \right), \quad (54)$$

where $\kappa = \pm \frac{\sqrt{kE_p(9E_p - 2\gamma^2)}}{2k\gamma}$ and $\omega = \frac{3}{2} \frac{pE}{\gamma}$. For distinct choices of integrating constant A , we obtain more soliton solutions. For the sake of smoothness, we have ignored herein the other solutions. In the subsequent section, we have depicted some graphical development of the mentioned solutions for realizing feasibility.

Graphical portrayal and interpretation

A plot is a graphical procedure for demonstrating a data set through the graph to express how two or more variables are related. To represent the nonlinear phenomena appropriately, graphical description is an important tool. This module contributes graphical depictions of the obtained results to the perturbed NLS equation with Kerr law nonlinearity and nonlinear dynamics of the radial dislocations in MTs. We develop ample soliton profiles by receiving different values of the existing unknowns of each result. The behaviors of the solutions are sketched in 3D and 2D contours which describes the mechanism of the illustrated wave profiles.

Interpretations of solutions to the perturbed NLS equation

The perturbed NLS equation deals with certain exact solutions which are accumulated in equations (15)-(32). The obtained solutions deliver a sort of wave structures by taking modulus plot like the kink soliton, flat kink soliton, compacton, bell shape soliton, anti-bell shape soliton, and other soliton shapes which have a significant feature in analyzing various types of nonlinear incidents. The kink soliton describes the propagation in fiber-optic communication which transmits information by transferring pulses of infrared light from one place to another through an optical fiber. The light is a form of carrier wave that is modulated to carry information. In addition, the analysis of compacton deals with a variety of nonlinear events, such as a cluster's hydrodynamic model, liquid drop fission and fusion mechanisms, super-deformed nuclei, etc. The delineation of the graphs of the solutions (16), (18), (22), (26) and (29) for the perturbed NLS equation are represented by the Figs. 1-10. The graphs of the other solutions have been ignored due to uniformity.

The solution (16) describes the kink soliton structure for $c = -2$ and other unknown values of $R = T = \beta = -2$. But, increasing the value of $c = -0.54$ and constant $\beta = -0.48$ represent a flat structured kink soliton. The 3D envelopes are sketched in Fig. 1 and Fig. 2 within the limit $-4 \leq x \leq 4, 1 < t \leq 4$ and 2D envelopes are sketched for $t = 0$.

The solution (18) represents the standard smooth kink soliton for the value $c = -0.06$ and other unknown values of $\beta = 2, R = T = -2$. This kind of shape travels from one asymptotic location to the next. On the other hand, the wave shape slightly changes for assigning the wave speed $c = 0.15$ and other unknown values of $\beta = -0.67, R = 1.09, T = 2$. The 3D envelopes are portrayed in Fig. 3 and Fig. 4 within the limit $-10 \leq x \leq 10, 2 < t \leq 10$ and 2D envelopes are shown for $t = 0$.

The solution (22) behaves the general soliton structure for $c = -0.01$ and other values of $A = -0.25, \beta = 1.97, R = T = -2$. When the wave speed increases to $c = 0.54$, and other values are $A = -0.23, \beta = 1.5, R = -2, T = -0.69$, we attain another soliton shape. The 3D envelopes are outlined in Fig. 5 and Fig. 6 within the limit $-0.5 \leq x \leq 0.5, 0 < t \leq 2$ and 2D envelopes are outlined for $t = 0$.

The solution (26) demonstrates bell-shaped soliton for $c = -1.24$ and other unknown values of $\beta = 0.03, R = -1.18, T = -0.90$. On the other hand, if the wave speed changes ($c = 1.21$) and other parameters remain unchanged, we receive the anti-bell shape soliton shown in Fig. 8. The 3D envelopes are presented in Fig. 7 and Fig. 8 within the limit $-10 \leq x \leq 10, 0 < t \leq 5$ and 2D envelopes are presented for $t = 0$.

Furthermore, the solution (26) reveals a significant wave profile entitled as compacton for the wave speed $c = 0.03$ and other unnamed values of $T = -0.90, \beta = 0.03, R = -1.18$. Compacton is a special type of wave structure with compact support where the nonlinear term confines to a finite core, thus the exponential wings disappear. The 3D envelope is shown in Fig. 9 within the boundary $-20 \leq x \leq 20, 0 < t \leq 10$ and 2D envelope is shown for $t = 0$. In contrast, if the wave speed is negative and other parameters are also negative ($\beta = -0.01, R = -0.73, T = -0.97$), we find a parabolic shape soliton profile. The 3D envelope is outlined in Fig. 10 within the boundary $-7 \leq x \leq 7, 0 < t \leq 5$ and 2D envelope is outlined for $t = 0$.

The solution (29) defines the plane kink type soliton for $c = -0.01$ and other values $A = -0.12, \beta = -0.54, R = -0.88, T = -0.90$. This shape of soliton started from the origin and later it moves parallel to the ground. Alternatively, the shape and direction change with respect to the positive wave velocity $c = 0.01$ and other unknown values $A = -0.12, \beta = -0.54, R = -0.88, T = -0.90$. The 3D envelopes are delineated in Fig. 11 and Fig. 12 within the limit $0 \leq x \leq 4, 0 < t \leq 3$ and 2D envelopes are delineated for $t = 0$.

The dynamics of the nonlinear radial dislocations in MTs

The nonlinear dynamics of the radial dislocations in MTs delivers a variety of exact solutions which are accumulated in equations (40)-(54). The obtained solutions deliver a sort of wave structures, like kink, flat kink, double soliton, and other shapes which have a significant feature in analyzing various nonlinear incidents. The delineation of the graphs of the solutions (40), (48) and (52) for the stated NLEE are represented by the Figs. 13-16. The graphs of the other solutions have been neglected due to uniformity.

The solution (40) implies the flat kink soliton profile corresponding to the wave speed $\omega = 0.39$ and other unidentified values $A = 1.26, \kappa = -0.01$. The shape of this wave ascends from right to left and later it travels with a constant velocity. But, only reducing the wave speed ($\omega = 0.15$), there is a small change of this shape arranged in Fig. 14. The 3D envelopes are portrayed in Fig. 13 and Fig. 14 within the limit $0 \leq x \leq -6, 0 < t \leq 5$ and 2D envelopes are portrayed for $t = 0$.

The solution (48) shows the standard kink soliton for the wave speed $\omega = 2$ and another unknown constant $\kappa = 0.03$. This shape moves from one infinitesimal state to another. Again, the wave speed $\omega = 0.92$ develops another type of kink soliton which is smoother than before. The 3D envelopes are sketched in Fig. 15 and Fig. 16 within the limit $-5 \leq x \leq -5, 0 < t \leq 4$ and 2D envelopes are sketched for $t = 0$.

Comparison of the results

In this module, the results acquired in this article are compared with the results deduced by other researchers.

Comparison of solutions of the perturbed NLS equation

In order to extract exact soliton solutions to the perturbed NLS equation, diverse academics used several solving approaches, as for instance, Zai-Yun et al. [32] investigated bell-shaped, kink and periodic soliton profiles along with a small number of solutions by taking the advantage of the bifurcation method. Eslami [33] examined the complex wave solutions and sketched only two graphs with the aid of direct algebraic scheme. But, in this article, the generalized Kudryashov scheme is adopted for determining scores of soliton solutions to the perturbed NLS equation with Kerr law nonlinearity and acquired kink, flat kink, smooth kink, bell-shaped, anti-bell shaped, compacton, parabolic and general type of solitons shown in the 3D and 2D graphics. The solutions of the perturbed NLS equation are compared in Table 1.

From Table 1, it is observed that Moosaei et al. [58] found only a few numbers of solutions in terms of tan and tanh functions. But we have established a large number of analytical solutions in this article related

to sinh, cosh, tanh, coth, sech functions presented in 2D and 3D graphical structures. It is important to note that the findings of this study are practical, compact size, meaningful, and easy to understand when it comes to nonlinear wave applications. It could also be used in plasma physics, semiconductor materials, heat pulse propagation in solids, nonlinear optical phenomena, etc.

Comparison of solutions of the nonlinear dynamics of the radial dislocations in MTs

Several studies investigated the nonlinear dynamics of radial dislocations in MTs using various schemes and established some exact solutions. For instance, Baskonus et al. [59] acquired a couple of rational solutions of tan and tanh functions by using the exponential function scheme. In this work, the generalized Kudryashov approach yields a range of solitary wave solutions for the nonlinear dynamics of radial dislocations including kink soliton, flat kink soliton and double soliton shapes which have a significant feature in studying various types of nonlinear incidents. In Table 2, the resultant solutions are compared to those obtained by Zdravkovic et al. [60] using the modified extended tanh function scheme.

It is noticed that Zdravkovic' et al. [60] found only tanh function solutions. On the other hand, we ascertain a sort of exact solutions incorporating sinh, cosh, coth and tanh functions that are distinctive and far-reaching. As a fundamental component of the cytoskeleton, the resulting solutions could interpret the mechanism of microtubules, particularly the cell nucleus and membrane. MTs are dynamical in the real field and in a stable state, the dimers of MTs are kept in straight position by PFs. When these dimers use hydrolyses energy, they become nonlinear and turn into kink-shaped excitations. These stimulated dimers, on the other hand, return to the starting stage with their own, as illustrated by the kink-shaped soliton.

Conclusion

The perturbed NLS equation with Kerr law nonlinearity and nonlinear dynamics of the radial dislocation in MTs have been investigated in this article through the generalized Kudryashov approach and in terms of hyperbolic, rational, and trigonometric functions, we have confirmed some broad-spectral, functional, and advanced soliton solutions. The obtained solutions have been compared to existing solutions that have already been found in the literature, and it is evident from this comparison that some of the obtained solutions are comparable to earlier findings and some solutions are distinct from others. In particular, the solutions (13), (20), (27), (39) and (50) are wide-spectrum and significant. Figurative representations of some of the obtained solutions, such as kink shaped profile, flat kink, compacton, bell-shaped profile, anti-bell shape, double soliton profile, and other soliton shapes, have been plotted in three- and two-dimensional format using independent values of the unknown parameters to demonstrate the compatibility of the solutions. The solutions have been validated using the computer algebra system for reliability by setting them into the main equations and confirming that they are correct. This study may be valuable for future research in terms of technique and precision of solutions, notably in solving NLEEs, which have a high level of efficacy in the nonlinear arena.

CRedit authorship contribution statement

M. Ali Akbar: Conceptualization, Methodology, Project administration, Supervision, Visualization, Writing – original draft. **Abdul-Majid Wazwaz:** Conceptualization, Methodology, Project administration, Supervision, Visualization. **Forhad Mahmud:** Data curation, Formal analysis, Investigation, Resources, Writing – review & editing. **Dumitru Baleanu:** Data curation, Funding acquisition, Project administration, Supervision. **Ripan Roy:** Methodology, Resources, Validation,

Writing – original draft. **Hemonta Kumar Barman:** Formal analysis, Investigation, Software, Validation. **W. Mahmoud:** Data curation, Resources, Visualization. **Mohammed A. Al Sharif:** Formal analysis, Funding acquisition, Investigation, Visualization, Writing – original draft. **M.S. Osman:** Conceptualization, Funding acquisition, Methodology, Resources, Software, Supervision, Validation, Writing – review & editing.

Declaration of Competing Interest

The authors declare that they have no known competing financial interests or personal relationships that could have appeared to influence the work reported in this paper.

Data availability

No data was used for the research described in the article.

Acknowledgement

The authors would like to thank the Deanship of Scientific Research at Umm Al-Qura University for supporting this work by Grant Code: (22UQU4410172DSR07).

Data Availability Statement

All data generated and analyzed during this study are included in this article.

References

- [1] Tarla S, Ali K, Yilmazer R, Osman MS. On dynamical behavior for optical solitons sustained by the perturbed Chen-Lee-Liu model. *Communications in Theoretical Physics*, 2022; 72: 075005.
- [2] Isozaki H. Maxwell equation: inverse scattering in electromagnetism. *World Scientific* 2018;1–30.
- [3] Polyanin AD, Zhurov AI. Exact solutions of linear and non-linear differential-difference heat and diffusion equations with finite relaxation time. *Int J Non Linear Mech* 2013;54:115–26.
- [4] Kayum MA, Ara S, Barman HK, Akbar MA. Soliton solutions to voltage analysis in nonlinear electrical transmission lines and electric signals in telegraph lines. *Results Phys*, 2020; 18: 103269.
- [5] Cherniha R, Davydovych V. Lie and conditional symmetries of the three-component diffusive Lotka-Volterra system. *J Phys A: Math Theoretical*, 2013; 46: 185204.
- [6] Az-Zo'bi E, Al-Maaitah AF, Tashtoush MA, Osman MS. New generalised cubic–quintic–septic NLSE and its optical solitons. *Pramana* 2022;96(4).
- [7] Vevek US, Namazi H, Haghghi R, Kulish VV. Analysis and validation of exact solutions to Navier-Stokes equation in connection with quantum fluid dynamics. *Mathematics in Engineering, Science & Aerospace* 2016;7(2):389–417.
- [8] Osman MS, Tariq KU, Bekir A, Elmoasry A, Elazab NS, Younis M, Abdel-Aty M. Investigation of soliton solutions with different wave structures to the (2+ 1)-dimensional Heisenberg ferromagnetic spin chain equation. *Communications in Theoretical Physics*. 2020; 72(3): 035002.
- [9] Akbar MA, Kayum MA, Osman MS, Abdel-Aty AH, Eleuch H. Analysis of voltage and current flow of electrical transmission lines through mZK equation. *Results in Physics*, 2021; 20: 103696.
- [10] Ismael HF, Akkili AN, Murad MA, Bulut H, Mahmoud W, Osman MS. Boiti–Leon–Manna–Pempinelli equation including time-dependent coefficient (vBLMPE): a variety of nonautonomous geometrical structures of wave solutions. *Nonlinear Dyn* 2022. <https://doi.org/10.1007/s11071-022-07817-5>.
- [11] Batool F, Rezazadeh H, Akinymi L, Inc M. New explicit soliton solutions for the generalized coupled integrable dispersionless system. *Opt Quant Electron* 2022;54(724):1–9.
- [12] Wang B-H, Wang Y-Y, Dai C-Q, Chen Y-X. Dynamical characteristic of analytical fractional solitons for the space-time fractional Fokas-Lenells equation. *Alexandria Eng J* 2020;59(6):4699–707.
- [13] Dai C-Q, Wang Y-Y, Zhang J-F. Managements of scalar and vector rogue waves in a partially nonlocal nonlinear medium with linear and harmonic potentials. *Nonlinear Dyn* 2020;102(1):379–91.
- [14] Ntiamoah D, Ofori-Atta W, Akinymi L. The higher-order modified Korteweg-de Vries equation: Its soliton, breather and approximate solutions. *J Ocean Eng Sci* 2022. <https://doi.org/10.1016/j.joes.2022.06.042> (in press).
- [15] Fang Y, Wu GZ, Wang YY, Dai CQ. Data-driven femtosecond optical soliton soliton excitations and parameters discovery of the high-order NLSE using the PINN. *Nonlinear Dyn* 2021;105:603–16.

- [16] Jaradat I, Alquran M, Sivasundaram S, Baleanu D. Simulating the joint impact of temporal and spatial memory indices via a novel analytical scheme. *Nonlinear Dyn* 2021;103(3):2509–24.
- [17] Gonzalez-Gaxiola O, Biswas A, Asma M, Alzahrani AK. Highly dispersive optical solitons with non-local law of refractive index by Laplace-Adomian decomposition. *Opt Quant Electron* 2021;53(1):55.
- [18] Khader MM, Saad KM, Hammouch Z, Baleanu D. A spectral collocation method for solving fractional KdV and KdV-Burgers equations with non-singular kernel derivatives. *Appl Numer Math* 2021;161:137–46.
- [19] Liu JG, Zhu WH, Osman MS, Ma WX. An explicit plethora of different classes of interactive lump solutions for an extension form of 3D-Jimbo-Miwa model. *Eur Phys J Plus* 2020;135(5):412.
- [20] Yousef HM, Abbas IA. Nonlinear generalized thermoelasticity: theory and application. *J Umm Al-Qura Univ Eng Architecture* 2022. <https://doi.org/10.1007/s43995-022-00006-w>.
- [21] Nisar KS, Alsallami SA, Inc M, Iqbal MS, Baber MZ, Tarar MA. On the exact solutions of nonlinear extended Fisher-Kolmogorov equation by using the He's variational approach. *Aims Mathematics* 2022;7(8):13874–86.
- [22] Akbulut A, Kaplan M, Tascan F. The investigation of exact solutions of nonlinear partial differential equations by using exp $(-\phi(\xi))$ method. *Optik-Int J Light Electron Optics* 2017;132:382–7.
- [23] Osman MS. Analytical study of rational and double-soliton rational solutions governed by the KdV-Sawada-Kotera-Ramani equation with variable coefficients. *Nonlinear Dyn* 2017;89(3):2283–9.
- [24] Haque M, Akbar MA, Osman MS. Optical soliton solutions to the fractional nonlinear Fokas-Lenells and paraxial Schrödinger equations. *Opt Quant Electron* 2022;54:764.
- [25] Yao SW, Behera S, Inc M, Rezaadeh H, Virdi JP, Mahmoud W, et al. Analytical solutions of conformable Drinfeld-Sokolov-Wilson and Boiti Leon Pempinelli equations via sine-cosine method. *Results Phys* 2022;42:105990.
- [26] Akinyemi L, Şenol M, Az-Zo'bi E, Veerasha P, Akpan U. Novel soliton solutions of four sets of generalized (2+1)-dimensional Boussinesq-Kadomtsev-Petviashvili-like equations. *Mod Phys Lett B* 2022;36(01).
- [27] Yépez-Martínez H, Pashrashid A, Gómez-Aguilar JF, Akinyemi L, Rezaadeh H. The novel soliton solutions for the conformable perturbed nonlinear Schrödinger equation. *Mod Phys Lett B* 2022;36(8):2150597.
- [28] Akinyemi L, Veerasha P, Ajibola SO. Numerical simulation for coupled nonlinear Schrödinger-Korteweg-de Vries and Maccari systems of equations. *Mod Phys Lett B* 2021;35(20):2150339.
- [29] Gomez CA, Rezaadeh H, Inc M, Akinyemi L, Nazari F. The generalized Chen-Lee-Liu model with higher order nonlinearity: optical solitons. *Opt Quant Electron* 2022;54(492):1–8.
- [30] Zai-Yun Z, Xiang-Yang G, De-Min Y, Ying-Hui Z, Xin-Ping L. A note on exact traveling wave solutions to the perturbed nonlinear Schrödinger equation with Kerr law nonlinearity. *Commun Theor Phys* 2012;57:764–70.
- [31] Shehata AR. The traveling wave solutions to the perturbed nonlinear Schrödinger equation and the cubic quintic Ginzburg Landau equation using the modified (G'/G) -expansion method. *Appl Math Comput* 2010;217:1–11.
- [32] Zhang ZY, Liu ZH, Miao XJ, Chen YZ. Qualitative analysis and travelling wave solutions for the perturbed nonlinear Schrödinger equation with Kerr law nonlinearity. *Phys Lett A* 2011;375:1275–80.
- [33] Eslami M. Solitary wave solutions for the perturbed nonlinear Schrödinger equation with Kerr law nonlinearity under the direct algebraic method. *Optik* 2015;126:1312–7.
- [34] Dai C-Q, Wang Y-Y. Coupled spatial periodic waves and solitons in the photovoltaic photorefractive crystals. *Nonlinear Dyn* 2020;102(3):1733–41.
- [35] Mahak N, Akram G. The modified auxiliary equation method to investigate solutions of the perturbed nonlinear Schrödinger equation with Kerr law nonlinearity. *Optik* 2020;207:164467.
- [36] Al-Ghafri KS, Krishnan EV, Biswas A. W-shaped and other solitons in optical nanofibers. *Results Phys*, 2021; 23: 103973.
- [37] Hosseini K, Matinfar M, Mirzazadeh M. Soliton solutions of high order nonlinear Schrödinger equations with different laws of nonlinearities. *Regular and Chaotic Dynamics* 2021;26(1):105–12.
- [38] Zdravković S, Satarčić MV, Maluckov A, Balaž A. A nonlinear model of the dynamics of radial dislocations in microtubules. *Appl Math Comput* 2014;237:227–37.
- [39] Alam N, Belgacem FBM. Microtubules nonlinear model dynamics investigations through the exp $(-\phi(\xi))$ expansion method implementation. *Mathematics* 2016;4:6.
- [40] Zdravkovic S, Zekovic S. Nonlinear dynamics of microtubules and series expansion unknown function method. *Chin J Phys* 2017;55(6):2400–6.
- [41] Zdravkovic S. Mechanical models of microtubules. Complexity in Biological and physical systems: Bifurcations, Solitons and Fractals, 2018.
- [42] Abdou MA. An analytical approach for space-time fractal order nonlinear dynamics of microtubules. *Waves Random Complex Medium* 2018;1517951.
- [43] Roy R, Akbar MA, Seadawy AR, Baleanu D. Search for adequate closed form wave solutions to space-time fractional nonlinear equations. *Partial Differential Equations in Applied Mathematics*, 2021; 3: 100025.
- [44] Justin M, Zdravković S, Hubert MB, Betchewe G, Doka SY, Kofane TC. Chaotic vibration of microtubules and biological information processing. *BioSystems*, 2020; 198: 104230.
- [45] Owayed S, Abdou MA, Abdel-Aty AH, Ibraheem AA, Nekhili R, Baleanu D. New optical soliton solutions of space-time fractional nonlinear dynamics of microtubules via three integration schemes. *J Intell Fuzzy Syst* 2020;38(3):2859–66.
- [46] Kudryashov NA. One method for finding exact solutions of nonlinear differential equations. *Communications in Nonlinear Science and Numerical Simulations* 2012;17(6):2248–53.
- [47] Akinyemi L, Mirzazadeh M, Badri SA, Hosseini K. Dynamical solitons for the perturbed Biswas-Milovic equation with Kudryashov's law of refractive index using the first integral method. *J Mod Opt* 2022;69(3):172–82.
- [48] Alam MN, Bonyah E, Al-Asad MF, Osman MS, Abualnaja KM. Stable and functional solutions of the Klein-Fock-Gordon equation with nonlinear physical phenomena. *Physica Scripta*, 2021; 96(5): 055207.
- [49] Barman HK, Seadawy AR, Akbar MA, Baleanu D. Competent closed form soliton solutions to the Riemann wave equation and the Novikov-Veselov equation. *Results in Physics*, 2020; 17: 103131.
- [50] Barman HK, Roy R, Mahmud F, Akbar MA, Osman MS. Harmonizing wave solutions to the Fokas-Lenells model through the Generalized Kudryashov method. *Optik*, 2021; 229: 166294.
- [51] Barman HK, Akbar MA, Osman MS, Nisar KS. Solutions to the Konopelchenko-Dubrovsky equation and the Landau-Ginzburg-Higgs equation via the generalized Kudryashov technique. *Results in Physics*, 2021; 24: 104092.
- [52] Khan K, Akbar MA. Solving unsteady Korteweg-de Vries equation and its two alternatives. *Math Methods Appl Sci* 2016;39(10):2752–60.
- [53] Zayed EME, Al-Nowehy AG. Exact travelling wave solutions for nonlinear PDEs in mathematical physics using the generalized Kudryashov method. *Serbian J Electr Eng* 2016;13(2):203–27.
- [54] Mahmud F, Samsuzzohsa M, Akbar MA. The generalized Kudryashov method to obtain exact traveling wave solutions of the PHI-four equation and the fisher equation. *Results Phys* 2017;7:4296–302.
- [55] Barman HK, Islam ME, Akbar MA. A study on the compatibility of the Generalized Kudryashov method to determine the wave solutions. *Propul Power Res* 2021;10(1):95–105.
- [56] Barman HK, Akter MS, Uddin MH, Akbar MA, Baleanu D, Osman MS. Physically significant wave solutions to the Riemann wave equations and the Landau-Ginzburg-Higgs equation. *Results in Physics*, 2021; 27: 104517.
- [57] Kudryashov NA, Kutukov AA, Lavrova SF, Safonova DV. On solutions of one of the second-order nonlinear differential equation: An in-depth look and critical review. *Optik-Int. J. Light and Electron Optics*, 255 (2022) 168674.
- [58] Moosaei H, Mirzazadeh M, Yildirim A. Exact solutions to the perturbed nonlinear Schrödinger equation with Kerr law nonlinearity by using the first integral method. *Nonlinear Anal Modell Control* 2011;16(3):332–9.
- [59] Baskonus HM, Cattani C, Ciancio A. Periodic, complex and kink-type solitons for the nonlinear model in microtubules. *Appl Sci* 2019;21:34–45.
- [60] Zdravković S, Satarčić MV, Sivčević V. General model of microtubules. *Nonlinear Dyn* 2018;92(2):479–86.